Magnetic-field-induced crossover of vortex-line coupling in SmFeAsO$_{0.85}$ single crystal

Hyun-Sook Lee,[1,*] Marek Bartkowiak,[2,†] Jun Sung Kim,[1] and Hu-Jong Lee[1,‡]

[1]*Department of Physics, Pohang University of Science and Technology, Pohang 790-784, Republic of Korea*
[2]*Hochfeld-Magnetlabor Dresden (HLD), Forschungszentrum Dresden–Rossendorf, Dresden, Germany*
(Received 25 June 2010; revised manuscript received 30 August 2010; published 28 September 2010)

We take the resistivity (ρ) and the current-voltage (I-V) characteristics of a SmFeAsO$_{0.85}$ single crystal as a function of temperature (T) for various magnetic fields up to 18 T along the c axis. The tail region of $\rho(T)$ well fits the three-dimensional (3D) vortex-glass critical behavior. The critical exponents for the vortex-glass scaling of $(d \ln \rho/dT)^{-1}$-T, I-V curves, and the thermal activation energies of vortices in magnetic fields show a crossover for magnetic fields around 3 T. The crossover behavior results from the change in the strength of the vortex pinning and the entanglement of vortex lines in the stacked superconducting structure of SmFeAsO$_{0.85}$ material with the c-axis vortex-line coupling lying in between highly anisotropic Bi-based cuprates with decoupled two-dimensional vortices and less-anisotropic YBa$_2$Cu$_3$O$_{7-\delta}$ with coupled 3D vortices.

I. INTRODUCTION

The resistive transition of recently discovered oxypnictides, REFeAsO$_{1-x}$F$_x$ (RE=rare-earth elements),[1] with high superconducting transition temperature (T_c), was reported to be broadened and tailed with increasing applied magnetic fields.[2–8] This feature is similar to that of high-T_c cuprates and is known to be due to strong thermal fluctuations that result from the high transition temperature, short coherence length, and large anisotropy. In the mixed state, thermal fluctuations directly affect the vortex motion by the thermally assisted flux flow (TAFF) and leads to the tail at the resistive transition. The magnitude of thermal fluctuations is quantified by the Ginzburg parameter,[9] $Gi=10^{-9}[\frac{\kappa^4 T_c[\mathrm{K}]\gamma^2}{H_{c2}(0)[\mathrm{Oe}]}]^2$, where $\kappa=\lambda_0/\xi_0$ is the Ginzburg-Landau parameter (λ_0 the London penetration depth, ξ_0 the superconducting coherence length), $H_{c2}(0)$ the zero-temperature upper critical field, and $\gamma = \xi_{ab}/\xi_c$ the anisotropy ratio ($\xi_{ab,c}$ the ab plane and the c-axis coherence length). $Gi \sim 1 \times 10^{-8}$–1×10^{-5} for conventional low-T_c superconductors while $Gi \sim 1 \times 10^{-2}$–1×10^{-1} for high-T_c cuprates.[9] Strong thermal fluctuations give a rich variety of vortex phases and vortex dynamics in high-T_c superconductors.

The Ginzburg parameter for thermal fluctuations in SmFeAsO$_{1-x}$F$_x$, with the highest $T_c(\sim 55$ K) among iron-based superconductors, are expected to be as high as $Gi \sim 1 \times 10^{-2}$.[5,7,10] The value of Gi of 1111-oxypnictides is comparable to that of cuprates because of a larger value of κ [for instance, $\kappa \simeq 110$ for NdFeAsO$_{1-x}$F$_x$ compared with $\kappa \simeq 85$ for YBa$_2$Cu$_3$O$_{7-\delta}$ (YBCO) (Ref. 10)] in spite of the lower value of T_c. Therefore, as in high-T_c cuprates, diverse phases and dynamics are expected in the vortex state of SmFeAsO$_{1-x}$F$_x$. The nature of the vortex matters in these layered superconductors is highly sensitive to the type and the density of defects. Therefore, the intrinsic vortex behavior of REFeAsO$_{1-x}$F$_x$ should be studied by using high-quality single crystals. But, the difficulty with the single-crystal growth of REFeAsO$_{1-x}$F$_x$ hinders the detailed study on the vortex properties in the material. To date, only three reports are available on the nature of the vortex state of NdFeAsO$_{1-x}$F$_x$ single crystals in the family of pnictides; two

reports by taking magnetic properties[11,12] and one by transport properties[2] of the material. However, details of the vortex phases and the dynamic properties of REFeAsO$_{1-x}$F$_x$ are still lacking.

In this paper, we present the vortex properties of a SmFeAsO$_{0.85}$ single crystal, including vortex dynamics and vortex phase diagram, based on electrical transport measurements. The sample resistivity ρ and current-voltage (I-V) characteristics of the SmFeAsO$_{0.85}$ single crystal were examined for various temperatures around T_c and c-axis magnetic fields up to 18 T. The temperature dependence of ρ and the I-V characteristics well fit the characteristics of the vortex-glass critical state. As in high-T_c cuprates, the vortex-glass-to-vortex-liquid phase transition takes place in a wide temperature range below the upper-critical-field line in the vortex-phase diagram. Crossing the magnetic field range around 3 T in the three-dimensional (3D) vortex regime, however, an unusual behavior was observed in the magnetic-field dependence of the critical exponent of the phase transition and in that of the thermal activation energy of the vortex motion. Similar crossover behavior in both the critical exponent and activation energy with increasing fields was also observed previously in the Bi-based cuprates (BSCCO) such as Bi$_2$Sr$_2$CaCu$_2$O$_{8+\delta}$ and Bi$_2$Sr$_2$Ca$_2$Cu$_3$O$_{10+\delta}$. The occurrence of the crossover of vortex character near H=3 T in SmFeAsO$_{0.85}$ indicates that the vortex lines of SmFeAsO$_{0.85}$ are coupled along the c axis like in YBCO but the detailed behavior more resembles the two-dimensional (2D)-like vortex behavior of BSCCO.

II. EXPERIMENT

SmFeAsO$_{0.85}$ single crystals with nominal compositions were grown under a high-temperature and high-pressure condition. Details of the single-crystal growth are described elsewhere.[13] The standard four-probe technique was used to measure ρ and the I-V characteristics of SmFeAsO$_{0.85}$ single crystals. For measurements, metallic (Au) leads were prepared on a flat surface of the sample (dimensions; $\sim 80 \times 50 \times 10 \ \mu\mathrm{m}^3$) by adopting the standard photolithographic-patterning technique (see the optical microscopic picture
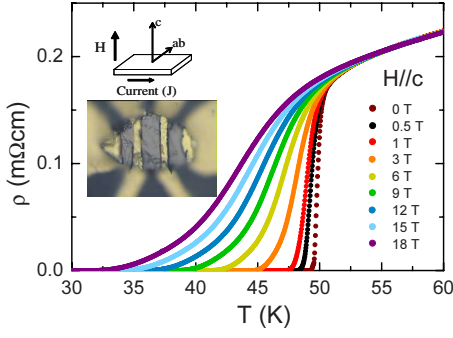
FIG. 1. (Color online) Temperature dependence of the resistivity $\rho(T)$ of a SmFeAsO$_{0.85}$ single crystal measured in the bias current density of 2×10^2 A/cm^2 for various c-axis magnetic fields up to 18 T. The inset illustrates the measurement configuration of the transport properties.

showing the sample configuration in the lower inset of Fig. 1). The contact resistance was about 1 Ω. Magnetic fields were applied in parallel with the crystallographic c axis while keeping it to be normal to the current flow (see the upper inset of Fig. 1). The in-plane resistivity was measured as a function of temperature in various magnetic fields up to 18 T for a dc bias current of 1 mA (or equivalently, for a current density of 2×10^2 A/cm^2). The bias level corresponds to an ohmic region. *I-V* measurements were carried out at different temperatures in the vortex-glass critical region in various fields from 0.5 to 6.9 T, with the bias current limited up to 20 mA to avoid the self-heating.

III. RESULTS AND DISCUSSION

Figure 1 shows the temperature dependence of the resistivity, $\rho(T)$, of a SmFeAsO$_{0.85}$ single crystal as magnetic fields (H) up to 18 T were applied along the c axis of the crystal. In zero field, the onset of the superconducting transition of the sample occurs around 50 K with a narrow transition width of $\sim$0.5 K, as determined by the criterion of 10–90 % of the normal-state resistivity (ρ_n). As the field increases, $\rho(T)$ curves become broader near the onset of the transition due to thermodynamic fluctuations of the superconducting order parameter. In addition, increasing fields, the tail in the resistivity just before reaching zero resistivity becomes more evident with a gradual extension to lower temperatures. Both broadening and tailing in $\rho(T)$ of SmFeAsO$_{0.85}$ with increasing fields are due to high thermal fluctuations. Similar tail of $\rho(T)$ in high c-axis fields also develops in layer-structured cuprates with stacked CuO$_2$ conducting planes and is known to be associated with the complex vortex dynamics.[14–17]

In Fig. 2(a), we analyze $\rho(T)$ of SmFeAsO$_{0.85}$ based on the theory of TAFF of vortices. In this regime, the resistivity is described by an Arrhenius behavior, $\rho \propto \exp[-U(H,T)/T]$, where U is the thermal-activation energy. As shown in Fig. 2(a), below 1% of $\rho_n[=\rho(55.5\ \text{K}) \approx 2 \times 10^{-4}\ \Omega\ \text{cm}]$, the resistivity as a function of $1/T$ follows an exponential dependence, as presented by the dotted lines. Similar behavior was observed in high-T_c cuprates[18,19] as well as in single-
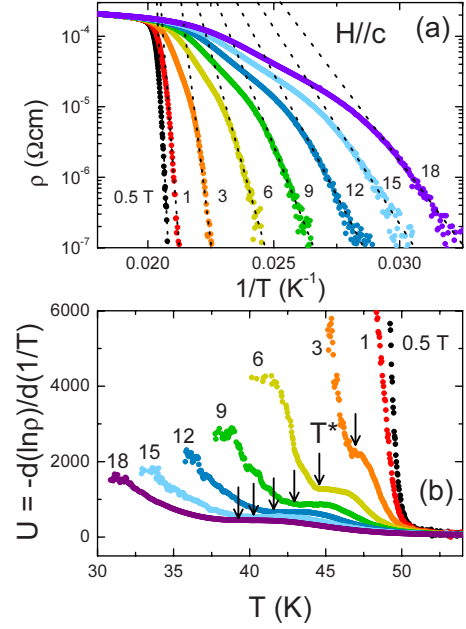
FIG. 2. (Color online) (a) An Arrhenius plot of the resistive transition of a SmFeAsO$_{0.85}$ single crystal in c-axis magnetic fields from 0.5 to 18 T. The dotted lines indicate logarithmic temperature variation in the low-resistivity part. (b) The temperature dependence of the activation energy, $U = -d(\ln \rho)/d(1/T)$, defined as the slope of the Arrhenius curves shown in Fig. 2(a). T^* marked by an arrow for each curve signifies the temperature of entering into the vortex-glass critical-state region.

crystalline pnictides of NdFeAsO$_{0.7}$F$_{0.3}$.[2] The slope of the Arrhenius plot of the curve $U = -d(\ln \rho)/d(1/T)$, or the activation energy, is presented as a function of temperature in Fig. 2(b). As temperature decreases, the slope of each curve starts fast increasing at a characteristic temperature (T^*), which signifies entering into the vortex-glass critical-state region as previously seen in high-T_c cuprates.[20,21]

Analyzing the temperature dependence of the sample resistivity $\rho(T)$ below T^*, one can confirm the presence of the vortex-glass state in SmFeAsO$_{0.85}$. According to a vortex-glass theory,[22] the resistivity vanishes at the vortex-glass temperature T_g following the relation of $R \sim |T-T_g|^{\nu(z+2-d)}$, where d is the sample dimensionality. Here, ν is the static exponent of the vortex-glass correlation length, $\xi_g \sim |T-T_g|^{-\nu}$, and z is the dynamic exponent for the correlation time $\tau_g \sim \xi_g^z$. We assume $d=3$ because ξ_g, estimated to be $\sim$20–80 nm at $0.1 \leq H \leq 7$ T for YBCO (Ref. 23) and $\sim$30 nm at $H=1$ T for Bi$_2$Sr$_2$Ca$_2$Cu$_3$O$_{10+\delta}$,[24] is much shorter than the sample thickness ($\sim$10 μm). Therefore, the logarithmic derivative of the resistivity is linearly dependent on T as

$$\left(\frac{d \ln \rho}{dT} \right)^{-1} = \frac{1}{s}(T - T_g) \tag{1}$$

with the slope being the inverse of $s = \nu(z-1)$. From the linear region of the $(d \ln \rho / dT)^{-1}$ vs T plot, we estimate T_g and the critical exponent s. As shown in Fig. 3, the resistivity of SmFeAsO$_{0.85}$ is well described by the vortex-glass picture in
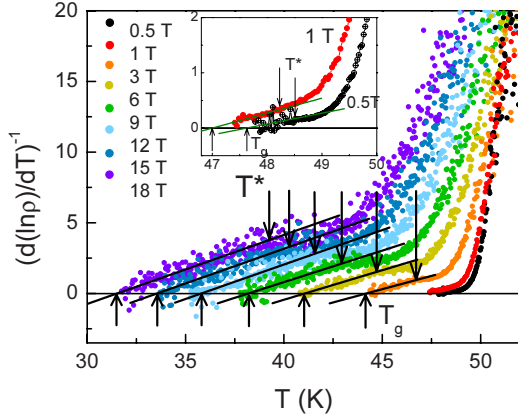
FIG. 3. (Color online) Inverse logarithmic derivative of resistivity for different fields. The solid lines represent fits to the vortex-glass theory by using the relation of Eq. (1). The glass temperature, T_g, is determined by the relation $(d \ln \rho/dT)^{-1}|_{T^*}=0$. T^* defines the upper temperature limit of the vortex-glass critical region, the slope of which gives the critical exponent $s=\nu(z-1)$ for each field. Inset is the magnified view of low-field data for 0.5 and 1 T.

the temperature range of $T_g < T < T^*$. The temperature (T^*) of a deviation from the linearity in this plot is the upper temperature limit of the critical region associated with the vortex-glass-to-vortex-liquid phase transition. The field dependence of the critical exponent, obtained from the best fit, is shown in Fig. 5 for the later analysis.

We also cross-check the transition from the vortex-glass-to-vortex-liquid phase in SmFeAsO$_{0.85}$ by using the I-V scaling. According to the vortex-glass theory, there are two different current and voltage regimes showing distinct I-V scalings, which follow the relation[25,26]

$$(V/I)\left|1-T/T_g(H)\right|^{\nu(d-2-z)} = F_{\pm}\left[(I/T)\left|1-T/T_g(H)\right|^{\nu(1-d)}\right],$$

$$(2)$$

where $F_+(F_-)$ is the scaling function for T above (below) T_g. Typical results of scaled I-V curves are shown for 1 T and 6.9 T in Figs. 4(a) and 4(b), respectively. All the curves collapse into two universal curves of Eq. (2) for $d=3$, one for $T>T_g(F_+)$ and another for $T<T_g(F_-)$, with the best-scaling values of T_g, ν, and z. Values of T_g, ν, and z are estimated by the following procedure. First, T_g is approximately estimated from the $\log(I)$-$\log(V)$ curves as the temperature at which the curvature changes from an upturn to a downturn character as represented by dotted lines in the insets of Figs. 4(a) and 4(b). Second, z is determined from the slope of the $\log(I)$-$\log(V)$ curve at $T=T_g$ by using the power-law behavior of $V \propto I^{(z+1)/(d-1)}$. Third, ν is estimated so as to obtain the optimal collapse of different-T sets of data to Eq. (2) as shown in the main panels of Figs. 4(a) and 4(b). In this optimization procedure of scaling, initially estimated values of T_g and z were usually required to be retuned only over a narrow range of ν. All the I-V curves between 0.5 and 6.9 T were well scaled by the vortex-glass picture. The best-scaling values of the critical exponents were $\nu=1-1.7$ and $z=3.4-4.8$.
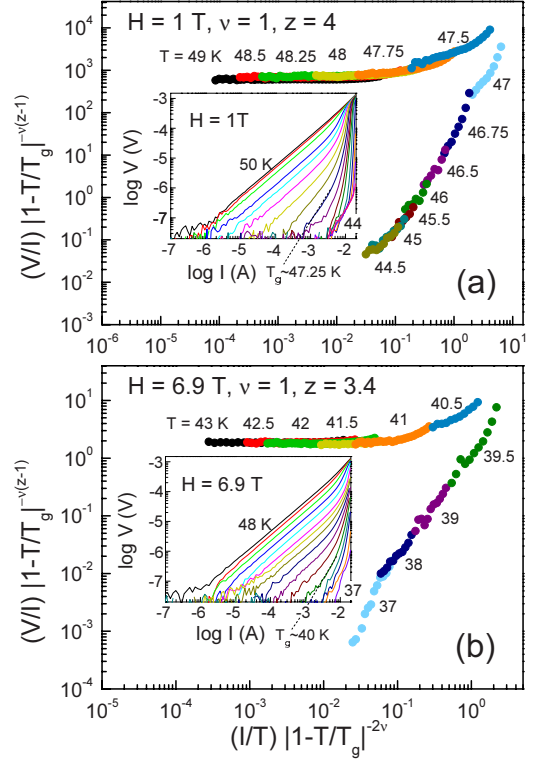
FIG. 4. (Color online) The vortex-glass scaling of I-V characteristics of SmFeAsO$_{0.85}$ by using Eq. (2). (a) Scaled I-V curves for $H=1$ T with the best-fit parameters of $T_g=47.25$ K, $\nu=1\pm0.1$, and $z=4\pm0.1$. In the I-V curves for $H=1$ T in the inset, the temperature ranges 44–46.5 K, 46.5–48.5 K, and 48.5–50 K with increments of 0.5 K, 0.25 K, and 0.5 K, respectively. (b) Scaled I-V curves for $H=6.9$ T with $T_g=40$ K, $\nu=1\pm0.1$, and $z=3.4\pm0.1$. In the I-V curves for $H=6.9$ T in the inset, the temperature ranges 37–39 K, 39–43 K, and 43–48 K with increments of 1 K, 0.5 K, and 1 K, respectively. I-V curves at T_g and T^* are denoted by dotted lines for each field.

In the I-V curve scaling, the critical exponents of ν and z are very sensitive to how optimally the I-V curves for different temperatures collapse on a single curve. Many different parameter sets were carefully tested for the scaling. But the I-V curves in various fields yield the best collapse for the values of ν and z presented above. All the values of $s=\nu(z-1)$ obtained from this scaling of I-V curves (Fig. 4) are summarized in Fig. 5, along with the exponents determined from the slope of $(d \ln \rho/dT)^{-1}$ vs T curve (Fig. 3). The values determined from these two different schemes are in good agreement with each other within the tolerance of errors although the $(d \ln \rho/dT)^{-1}$-T data for 0.5 T show larger fluctuations. The critical exponent s keeps decreasing with increasing magnetic fields. According to a theory,[9] a 3D vortex glass is in a universal class with s value in the range of $s\approx2.7-8.5$. The lower limit of the predicted exponent is denoted by the dotted line in Fig. 5. Values of the exponent s of our sample below 3 T are in the range predicted by the 3D vortex-glass theory but those above 3 T deviate from the 3D vortex-glass behavior. This indicates that the vortex-glass state of SmFeAsO$_{0.85}$ in the two field ranges (below and above 3 T) of the critical region is not in an identical universal class.
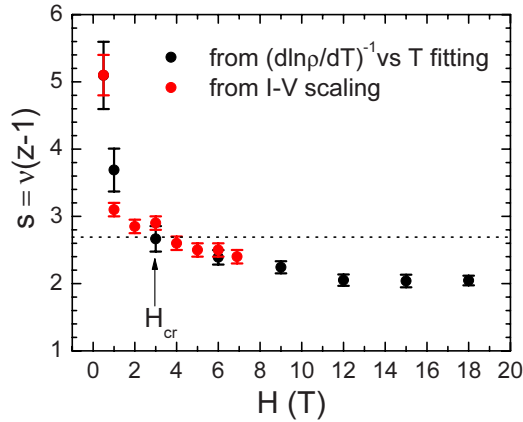
FIG. 5. (Color online) The critical exponents $s = \nu(z-1)$ for different fields, obtained from the vortex-glass scaling with $(d \ln \rho / dT)^{-1}$ vs T curves shown in Fig. 3 and I-V curves shown in Fig. 4. The dotted line indicates the lower limit of $s(\approx 2.7\text{–}8.5)$, predicted by the 3D vortex-glass picture (Ref. 9). The crossover field of H_{cr} is designated as the field of deviation from the expected 3D value.

The unusual behavior of the critical exponent s, such as the field dependence and the deviation from the predicted range of values, was also observed in high-T_c cuprates. For highly anisotropic $Bi_2Sr_2CaCu_2O_{8+\delta}$ single crystals[20] and $Bi_2Sr_2Ca_2Cu_3O_{10+\delta}$ thin films,[27] a reduction in the critical exponent s was observed near the crossover field (1–2 T) from a 3D to a 2D vortex-glass phase. YBCO, with the 3D vortex nature, reveals similar unusual behavior of the vortex-glass phases in following two cases. One is near the coexistence point of the vortex-glass and the Bose-glass phases.[28–30] The Bose-glass phase in YBCO single crystals develops when the field is applied in parallel with twin planes[28,29] or columnar defects.[30] Another case appears near the multicritical point (6–10 T) where the lattice-to-liquid (melting), the glass-to-liquid (glass), and the lattice-to-glass (peak effect) vortex phase transitions meet at a single phase point.[31,32]

We compare the behavior of the vortex-glass state of $SmFeAsO_{0.85}$ with that of high-T_c cuprates. The dimensional-crossover field is estimated by the relation of $H_{2D} \sim 4\Phi_0/(\gamma\delta)^2$, where γ is the effective-mass anisotropy ratio and δ is the interlayer distance between conducting layers.[20,27] For $Bi_2Sr_2CaCu_2O_{8+\delta}$, the values of $\gamma = 60\text{–}200$ and $\delta = 1.5$ nm give $H_{2D} = 0.1\text{–}1$ T. However, $\gamma = 5\text{–}10$ and $\delta = 0.84$ nm for $SmFeAsO_{0.85}$ lead to $H_{2D} = 100\text{–}500$ T. Thus, a 2D vortex field regime is not accessible in $SmFeAsO_{0.85}$ in the practical measurement field range of $H < \sim 100$ T. This finding is consistent with our recent result of c-axis transport measurements on $SmFeAsO_{0.85}$ single crystals, where the material shows bulk interlayer-coupling characteristics.[33] Therefore, it is unlikely that the 3D-2D crossover causes the unusual vortex-glass behavior near $H \sim 3$ T in our $SmFeAsO_{0.85}$ single crystal. We also rule out the mixture of vortex-glass and Bose-glass phases, because the disorder of points defects, possibly originating from oxygen vacancies in $SmFeAsO_{0.85}$ for c-axis fields, cannot be strongly correlated as in twinned[28,29] and irradiated[30] YBCO single crystals. Moreover, the possible existence of the mul-
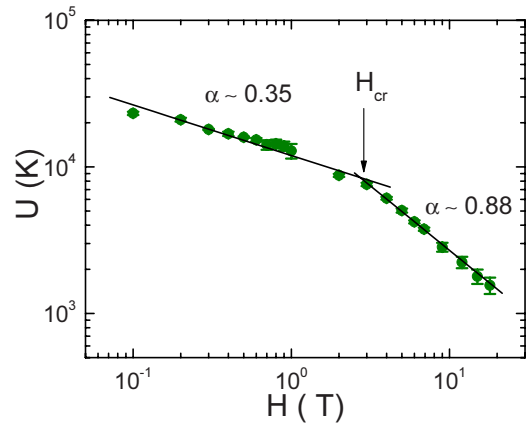
FIG. 6. (Color online) Field dependence of the activation energy $U(H)$, obtained from the slope of the Arrhenius plot in Fig. 2(a). The solid lines are fits to $U(H) \sim H^{-\alpha}$ with $\alpha \approx 0.35$ ($\alpha \approx 0.88$) below (above) the crossover field of $H_{cr}(\approx 3$ T).

ticritical point as observed in optimally doped YBCO is discounted in $SmFeAsO_{0.85}$ because the melting and the peak effect were not observed in the field range of our transport measurements. Although the peak effect was observed in $SmFeAsO_{0.8}F_{0.2}$ wires,[34] it occurred far below the irreversibility field line. Thus, the unusual field dependence of the critical exponent (s) and the deviation from the predicted range ($s \approx 2.7\text{–}8.5$) for a 3D vortex glass in $SmFeAsO_{0.85}$ indicate that the vortex nature of $SmFeAsO_{0.85}$ is quite distinct from those of two representative high-T_c cuprates, i.e., YBCO and BSCCO.

We further examine the nature of the unusual behavior of the critical exponent in $SmFeAsO_{0.85}$ by investigating the field dependence of the thermal activation energy $U(H)$, estimated from the linear slope of the Arrhenius plot in Fig. 2(a). Figure 6 shows the field dependence of U in a log-log plot. The activation energy of $SmFeAsO_{0.85}$ follows a power-law relation of $U(H) \sim H^{-\alpha}$ with different values of α; 0.35 for $H < 3$ T; and 0.88 for $H > 3$ T. The demarcating field value turns out to be close to the crossover field showing the above-mentioned unusual vortex-glass behavior. The abrupt change in the exponent α is consistent with what was reported in $NdFeAsO_{0.7}F_{0.3}$ single crystals.[2] Such a crossover behavior was also observed in highly anisotropic BSCCO (Refs. 18 and 35–38) and multilayered Mo/Si,[39] but not in less anisotropic YBCO.[14,17,21,40–42] The crossover in the value of activation-energy exponent α in highly anisotropic superconductors was explained by the dimensional crossover of vortices.[35,37,39] However, as discussed above, the crossover observed in $SmFeAsO_{0.85}$ is unlikely the dimensional crossover and other explanation is required.

The field dependence of U of the form $U \sim H^{-\alpha}$ is not well understood. It should be pointed out that the reduction in U of the form $U \sim H^{-\alpha}$ in high magnetic fields cannot be explained by the collective (elastic) creep theory,[9] in which an increase in U is predicted in high magnetic fields.[41,43–45] The behavior of $U \sim H^{-\alpha}$ can be explained by the plastic creep theory.[46–48] According to the *plastic-flux-creep model*,[46–48] the activation energy follows the form of $U \sim H^{-0.5}$, which is associated with the plastic deformation and

the entanglement of vortices in *weakly pinned vortex liquid* due to the presence of point defects. The motion of the vortices relative to each other in such an entangled liquid is significantly modified by cutting and reconnecting of the vortex lines.[47] A plastic-creep activation energy of the form of $U \sim H^{-0.7}$ was obtained in untwinned YBCO single crystals for high fields above the melting transition.[17] The faster reduction in U with H was suggested to be due to the *strongly pinned and entangled vortex liquid* around point defects, which induce lateral vortex wandering.[17]

From this point of view, we consider that point defects in $SmFeAsO_{0.85}$ play an important role and lead to a weakly (strongly) entangled liquid in low (high) fields. The plastic deformation and entanglement of vortex lines with increasing field in $SmFeAsO_{0.85}$ can lead to the reduced correlation length along vortex lines, i.e., weakening of vortex-line coupling and the resulting reduced activation energy. Based on these results, the characteristic field in $U \sim H^{-\alpha}$ observed in $SmFeAsO_{0.85}$ does not correspond to the 3D-to-2D dimensional crossover observed in BSCCO, but it is the field beyond which the entanglement of vortex lines gets stronger. This behavior has never been observed in YBCO. Weakening of the vortex-line coupling was also seen in measurements of the magnetic relaxation rate in $NdFeAsO_{0.9}F_{0.1}$ single crystals.[12]

By analyzing the unusual behavior of the critical exponent in vortex-glass scaling and the field dependence of the activation energy, we find that the vortex lines of $SmFeAsO_{0.85}$ are coupled along c-axis like YBCO, but the details of the vortex behavior are very different from those of YBCO showing 3D character. In some aspects, the vortex behaviors of $SmFeAsO_{0.85}$ resemble the 2D features in BSCCO. Further studies are required to clarify the origin of the different vortex behaviors between $SmFeAsO_{0.85}$ and YBCO because the vortex nature is sensitive not only to the type and density of defects but also to the vortex core properties that are determined by the Fermi-surface topology. The 2D-like behavior of vortices in $SmFeAsO_{0.85}$ may come from the quasi-two-dimensional Fermi-surface topology.

In Fig. 7, we present a vortex phase diagram of $SmFeAsO_{0.85}$ with different dynamic characteristics. It is similar to the phenomenological phase diagram for the high-T_c superconductors including the effects of thermal fluctuations and of quenched disorder (pinning). The upper critical field of H_{c2} is denoted by a solid line, which is extracted from 90% of ρ_n. As often observed in high-T_c cuprates, a vortex-glass-to-vortex-liquid phase transition is found in our $SmFeAsO_{0.85}$ single crystal in a wide temperature range well below H_{c2}. The characteristics field H_g of the vortex-glass phase transition, obtained from the $(d \ln \rho/dT)^{-1}$ vs T and I-V curves, are presented by the solid-and the open-diamond symbols, respectively, which are consistent with each other. The upper field limit of the critical region associated with the vortex-glass-to-vortex-liquid phase transition, H^*, is presented by open-circle symbols. The H^* divides the vortex-liquid phase into pinned liquid and unpinned liquid phases. According to the magnetic-field dependences of the critical exponents (Fig. 5) and the activation energy (Fig. 6), a crossover field of $H_{cr} \sim 3$ T exists in $SmFeAsO_{0.85}$, which is denoted by a dotted line in the criti-
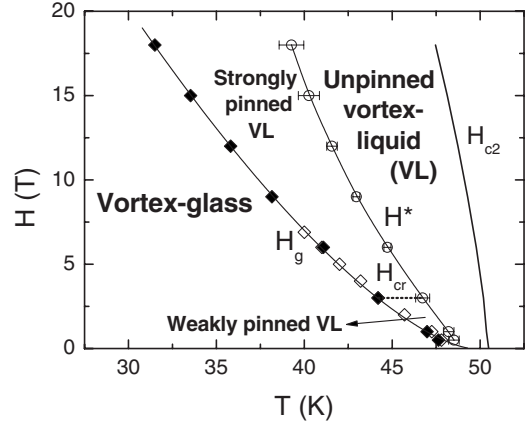
FIG. 7. Static vortex phase diagram of $SmFeAsO_{0.85}$. The solid line is the upper critical field (H_{c2}), estimated from 90% of the normal-state resistivity. The characteristics field H_g for vortex-glass-to-liquid transition are presented by solid- and open-diamond symbols as determined from $(d \ln \rho/dT)^{-1}$ vs T (Fig. 3) and I-V scaling (Fig. 4), respectively. The upper-field limit of the critical region associated with the vortex-glass-to-vortex-liquid phase transition, H^*, is indicated by open-circle symbols. The crossover field H_{cr} (≈ 3 T), denoted by a dotted line, is determined by the field dependence of the critical exponent (Fig. 5) and the activation energy (Fig. 6).

cal region of the glass-to-liquid transition in Fig. 7. From the analysis of the field-dependent activation energy we find the pinned vortex-liquid phases with different dynamical characteristics; weakly (strongly) pinned liquid for $H < H_{cr}$ (for $H > H_{cr}$).

IV. SUMMARY

Based on the vortex-glass theory, we investigated a three-dimensional vortex-glass-to-vortex-liquid transition in a $SmFeAsO_{0.85}$ single crystal by the variation in the slope of $(d \ln \rho/dT)^{-1}$ vs T curve and the I-V-curve scaling for different c-axis fields up to 18 T. As in layered cuprates, a broad vortex-liquid region is present in $SmFeAsO_{0.85}$ below the upper-critical field line in the vortex-phase diagram. The magnetic field dependence of the critical exponents for vortex-glass scaling indicates that the universal class of the vortex-glass state of $SmFeAsO_{0.85}$ changes crossing the field of ~ 3 T. The field dependence of the thermal activation energy also shows that the vortex-liquid phase consists of two dynamically different states, one with the characteristics of weak entanglement in the low-field range and another with the strong entanglement including lateral vortex wandering in the high-field range, caused by effective intrinsic pinning at point defects. The crossover behavior in $SmFeAsO_{0.85}$ is brought about by the field-induced change in the vortex-line coupling and the resulting change in the vortex-line pinning and entanglement rather than by the field-induced dimensional crossover of the vortex lines. Similar crossover in the vortex coupling along the c axis with increasing fields appears in highly anisotropic BSCCO ($H_{2D} = 0.1 - 1$ T) as vortex lines are decoupled into pancake vortices. In $SmFeAsO_{0.85}$, while the anisotropy is compa-

rable to YBCO, the vortex-line coupling more resembles the 2D-like vortex behavior of BSCCO. Thus, $SmFeAsO_{0.85}$ single crystals provide a convenient system to study the diverse vortex phases existing in layered superconducting materials.

*Present address: Korea Institute of Science and Technology, Seoul 136-791, Republic of Korea.

†Present address: Paul Scherrer Institut, WLGA/U127 5232 Villigen PSI, Switzerland.

‡Corresponding author; hjlee@postech.ac.kr

[1] Y. Kamihara, T. Watanabe, M. Hirano, and H. Hosono, J. Am. Chem. Soc. **130**, 3296 (2008).

[2] J. Jaroszynski, F. Hunte, L. Balicas, Y.-j. Jo, I. Raičević, A. Gurevich, D. C. Larbalestier, F. F. Balakirev, L. Fang, P. Cheng, Y. Jia, and H. H. Wen, Phys. Rev. B **78**, 174523 (2008).

[3] J. Karpinski, N. D. Zhigadlo, S. Katrych, Z. Bukowski, P. Moll, S. Weyeneth, H. Keller, R. Puzniak, M. Tortello, D. Daghero, R. Gonnelli, I. Maggio-Aprile, Y. Fasano, O. Fischer, and B. Batlogg, Physica C **469**, 370 (2009).

[4] Y. Jia, P. Cheng, L. Fang, H. Luo, H. Yang, C. Ren, L. Shan, C. Gu, and H.-H. Wen, Appl. Phys. Lett. **93**, 032503 (2008).

[5] J. Jaroszynski S. C. Riggs, F. Hunte, A. Gurevich, D. C. Larbalestier, G. S. Boebinger, F. F. Balakirev, A. Migliori, Z. A. Ren, W. Lu, J. Yang, X. L. Shen, X. L. Dong, Z. X. Zhao, R. Jin, A. S. Sefat, M. A. McGuire, B. C. Sales, D. K. Christen, and D. Mandrus, Phys. Rev. B **78**, 064511 (2008).

[6] H. Yang, C. Ren, L. Shan, and H.-H. Wen, Phys. Rev. B **78**, 092504 (2008).

[7] I. Pallecchi, C. Fanciulli, M. Tropeano, A. Palenzona, M. Ferretti, A. Malagoli, A. Martinelli, I. Sheikin, M. Putti, and C. Ferdeghini, Phys. Rev. B **79**, 104515 (2009).

[8] H.-S. Lee, M. Bartkowiak, J.-H. Park, J.-Y. Lee, J.-Y. Kim, N.-H. Sung, B. K. Cho, C.-U. Jung, J. S. Kim, and H.-J. Lee, Phys. Rev. B **80**, 144512 (2009).

[9] G. Blatter, M. V. Feigel'man, V. B. Geshkenbein, A. I. Larkin, and V. M. Vinokur, Rev. Mod. Phys. **66**, 1125 (1994).

[10] J. Kacmarcik, C. Marcenat, T. Klein, Z. Pribulova, C. J. van der Beek, M. Konczykowski, S. L. Budko, M. Tillman, N. Ni, and P. C. Canfield, Phys. Rev. B **80**, 014515 (2009).

[11] Z. Pribulova, T. Klein, J. Kacmarcik, C. Marcenat, M. Konczykowski, S. L. Bud'ko, M. Tillman, and P. C. Canfield, Phys. Rev. B **79**, 020508(R) (2009).

[12] R. Prozorov, M. E. Tillman, E. D. Mun, and P. C. Canfield, New J. Phys. **11**, 035004 (2009).

[13] H.-S. Lee, J.-H. Park, J.-Y. Lee, J.-Y. Kim, N.-H. Sung, T.-Y. Koo, B. K. Cho, C.-U. Jung, S. Saini, S.-J. Kim, and H.-J. Lee, Supercond. Sci. Technol. **22**, 075023 (2009).

[14] A. K. Pradhan, M. Muralidhar, Y. Feng, M. Murakami, K. Nakao, and N. Koshizuka, Phys. Rev. B **64**, 172505 (2001).

[15] H. Safar, P. L. Gammel, D. A. Huse, D. J. Bishop, W. C. Lee, J. Giapintzakis, and D. M. Ginsberg, Phys. Rev. Lett. **70**, 3800 (1993).

[16] J. A. Fendrich, W. K. Kwok, J. Giapintzakis, C. J. van der Beek, V. M. Vinokur, S. Fleshler, U. Welp, H. K. Viswanathan, and G. W. Crabtree, Phys. Rev. Lett. **74**, 1210 (1995).

[17] D. López, L. Krusin-Elbaum, H. Safar, E. Righi, F. de la Cruz, S. Grigera, C. Feild, W. K. Kwok, L. Paulius, and G. W. Crabtree, Phys. Rev. Lett. **80**, 1070 (1998).

[18] T. T. M. Palstra, B. Batlogg, L. F. Schneemeyer, and J. V. Waszczak, Phys. Rev. Lett. **61**, 1662 (1988).

[19] T. T. M. Palstra, B. Batlogg, R. B. van Dover, L. F. Schneemeyer, and J. V. Waszczak, Phys. Rev. B **41**, 6621 (1990).

[20] H. Safar, P. L. Gammel, D. J. Bishop, D. B. Mitzi, and A. Kapitulnik, Phys. Rev. Lett. **68**, 2672 (1992).

[21] Z. Sefrioui, D. Arias, E. M. Gonzalez, C. Leon, J. Santamaria, and J. L. Vicent, Phys. Rev. B **63**, 064503 (2001).

[22] M. P. A. Fisher, Phys. Rev. Lett. **62**, 1415 (1989).

[23] N.-C. Yeh, W. Jiang, D. S. Reed, U. Kriplani, and F. Holtzberg, Phys. Rev. B **47**, 6146 (1993).

[24] Q. Li, H. J. Wiesmann, M. Suenaga, L. Motowidlow, and P. Haldar, Phys. Rev. B **50**, 4256 (1994).

[25] D. S. Fisher, M. P. A. Fisher, and D. A. Huse, Phys. Rev. B **43**, 130 (1991).

[26] R. H. Koch, V. Foglietti, W. J. Gallagher, G. Koren, A. Gupta, and M. P. A. Fisher, Phys. Rev. Lett. **63**, 1511 (1989).

[27] P. Wagner, U. Frey, F. Hillmer, and H. Adrian, Phys. Rev. B **51**, 1206 (1995).

[28] S. A. Grigera, E. Morre, E. Osquiguil, C. Balseiro, G. Nieva, and F. de la Cruz, Phys. Rev. Lett. **81**, 2348 (1998).

[29] T. Naito, H. Iwasaki, T. Nishizaki, and N. Kobayashi, Phys. Rev. B **70**, 014515 (2004).

[30] W. Jiang, N.-C. Yeh, D. S. Reed, U. Kriplani, D. A. Beam, M. Konczykowski, T. A. Tombrello, and F. Holtzberg, Phys. Rev. Lett. **72**, 550 (1994).

[31] T. Nishizaki, T. Naito, S. Okayasu, A. Iwase, and N. Kobayashi, Phys. Rev. B **61**, 3649 (2000).

[32] K. Shibata, T. Nishizaki, T. Sasaki, and N. Kobayashi, Phys. Rev. B **66**, 214518 (2002).

[33] J.-H. Park, H.-S. Lee, B. K. Cho, Y.-H. Doh and H.-J. Lee (unpublished).

[34] Y. L. Chen, Y. J. Cui, Y. Yang, Y. Zhang, L. Wang, C. H. Cheng, C. Sorrell, and Y. Zhao, Supercond. Sci. Technol. **21**, 115014 (2008).

[35] J. T. Kucera, T. P. Orlando, G. Virshup, and J. N. Eckstein, Phys. Rev. B **46**, 11004 (1992).

[36] J. Mirković, K. Kimura, and K. Kadowaki, Phys. Rev. Lett. **82**, 2374 (1999).

[37] Y. Z. Zhang, Z. Wang, X. F. Lu, H. H. Wen, J. F. de Marneffe, R. Deltour, A. G. M. Jansen, and P. Wyder, Phys. Rev. B **71**, 052502 (2005).

[38] X. L. Wanga, A. H. Li, S. Yu, S. Ooi, K. Hirata, C. T. Lin, E. W. Collings, M. D. Sumption, M. Bhatia, S. Y. Ding, and S. X. Dou, J. Appl. Phys. **97**, 10B114 (2005).

[39] N. Ya. Fogel, V. G. Cherkasova, O. A. Koretzkaya, and A. S. Sidorenko, Phys. Rev. B **55**, 85 (1997).

[40] S. Zhu, D. K. Christen, C. E. Klabunde, J. R. Thompson, E. C. Jones, R. Feenstra, D. H. Lowndes, and D. P. Norton, Phys. Rev. B **46**, 5576 (1992).

[41] Y. Abulafia, A. Shaulov, Y. Wolfus, R. Prozorov, L. Burlachkov, Y. Yeshurun, D. Majer, E. Zeldov, H. Wuhl, V. B. Geshkenbein, and V. M. Vinokur, Phys. Rev. Lett. **77**, 1596 (1996).

[42] Xu Xiaojun, Fu Lan, Wang Liangbin, Zhang Yuheng, Fang Jun, Cao Xiaowen, Li Kebin, and Sekine Hisashi, Phys. Rev. B **59**, 608 (1999).

[43] H. Küpfer, S. N. Gordeev, W. Jahn, R. Kresse, R. Meier-Hirmer, T. Wolf, A. A. Zhukov, K. Salama, and D. Lee, Phys. Rev. B **50**, 7016 (1994).

[44] A. A. Zhukov, H. Kupfer, G. Perkins, L. F. Cohen, A. D. Caplin, S. A. Klestov, H. Claus, V. I. Voronkova, T. Wolf, and H. Wuhl, Phys. Rev. B **51**, 12704 (1995).

[45] G. K. Perkins, L. F. Cohen, A. A. Zhukov, and A. D. Caplin, Phys. Rev. B **51**, 8513 (1995).

[46] V. B. Geshkenbein, M. V. Feigel'man, A. I. Larkin, and V. M. Vinokur, Physica C **162-164**, 239 (1989).

[47] V. M. Vinokur, M. V. Feigel'man, V. B. Geshkenbein, and A. I. Larkin, Phys. Rev. Lett. **65**, 259 (1990).

[48] J. Kierfeld, H. Nordborg, and V. M. Vinokur, Phys. Rev. Lett. **85**, 4948 (2000).